



PREDICTION OF INTERLAMINAR STRESSES ACTING IN THE ANGLE PLY E-GLASS EPOXY COMPOSITES USING ANALYTICAL AND NUMERICAL METHODS

Mano Karthick R¹, Mohammed Asik S¹ and *Arul Marcel Moshi A²

¹Department of Mechanical Engineering, National Engineering College, Kovilpatti, Tamil Nadu– 628503, India

²Department of Mechanical Engineering, JKKN College of Engineering and Technology, Komarapalayam, Tamil Nadu-638183, India

Abstract

Prediction of interlaminar stress is the leading research area in the field of composite structures nowadays. Many research works related to the interlaminar stresses induced in the composite structures, such as the formulation of analytical solutions to predict the interlaminar stresses, finding out the additional provision to be made in the experimental set-up for the measurement of interlaminar stress, and the development of various theories for the accurate determination of inter-laminar stresses and free edge stresses are going on. Among the research works carried out so far, cross-ply composites have been concentrated more because of their more application areas. The present work considers an angle ply E-Glass epoxy composite structure for the interlaminar stress analysis. Interlaminar stresses induced in the considered angle ply composite for the given loading condition have been predicted using analytical and numerical analyses, and the results have been compared.

Keywords: *Free edge stress; Inter-laminar stress; Angle ply composite structure.*

1. Introduction

The free edge effects are due to the discontinuous change of elastic material properties in the adjacent layers of the laminate. Inter-laminar stresses near the free edges can be controlled to an extent through the choice of materials, fibre orientations, stacking sequence, layer thickness and the use of functionally graded materials [1]. However, the inter-laminar stresses in the vicinity of free edges can be eliminated completely locally by using a homogeneous material. The reinforcement technique's suppression of inter-laminar stresses near the free edge is costly. This technique provides a restraint against delamination due to inter-laminar stress but is not a complete solution [2].

Most of the composite laminate analysis uses the CLPT. CLPT assumes a planar state of stress along with the kinematic assumptions resulting from Kirchhoff's assumptions [3]. The determination of transverse stresses is not possible. Further, the CLPT is inadequate in determining the inter-laminar stresses. The transverse stresses become significant in the case of thick laminates under transverse loading. Further, these stresses are significant in case of geometric discontinuities like re-entrant corners, cut-outs, notches, ply-drops and material discontinuity as in the interfaces

near the free edges. Thus, the state of stress in such regions is highly three-dimensional and decays very fast inside the laminate [4].

Tahani et al. had used a layer-wise theory to investigate analytically the inter-laminar stresses near the free edges of general cross-ply composite laminates under uniform axial extension [5]. Tahani had developed two laminated beam theories for beams with general lamination within the displacement field of a layer-wise theory [6]. Nosier et al. had developed an analytical method to accurately calculate the inter-laminar stresses near the free edges of generally laminated composite plates under extension, by starting from the reduced elasticity displacement field for a long flat laminate [7].

Sarvestani et al. had established an analytical method to exactly obtain the interlaminar stresses near the free edges of generally laminated composite plates under the extension and bending. The constant parameters, which describe the global deformation of a laminate, are properly computed utilizing the improved first-order shear deformation theory [8]. Kant et al. had analyzed A simple C⁰ isoparametric finite element formulation based on a set of higher-order displacement models to analyse symmetric and asymmetric multilayered composite and sandwich beams subjected to sinusoidal loading. A computer algorithm has been developed which incorporates a realistic prediction of

*Corresponding Author - E- mail: moshibeo2010@gmail.com

transverse interlaminar stresses from equilibrium equations [9]. Lindemann et al. had presented a boundary finite element method as a very efficient numerical method using an example of a symmetric $[0^\circ/90^\circ]_s$ cross-ply laminate, which combines the advantages of the finite element method and the boundary element method [10]. Tahani et al. had determined the interlaminar stresses resulting from the bending of rectangular cross-ply composite laminates using a layer-wise laminate theory. The results indicated the presence of significant interlaminar stresses near the free edges [11]. Kant et al. had assessed a complete analytical model, which incorporates shear deformation as well as transverse normal thermal strains for the thermal stress analysis of cross-ply laminates subjected to linear or gradient thermal profiles across the thickness of the laminate. Numerical results of displacements and stresses were compared with three-dimensional (3D) elasticity solutions and other two-dimensional (2D) models [12].

From the literature survey, the need to evaluate the interlaminar stress and free-edge stress induced in the composite laminates was understood. In the present work, CLPT and HLPT formulations have been made to predict the interlaminar stress and free-edge stress induced in an angle ply composite structure. The results of the analytical study have been verified by carrying out a numerical analysis using ANSYS software.

2. Materials and Methods

A composite specimen was considered consisting of fibre material as E-Glass and matrix material as epoxy resin with the ply orientations of $[0/30/60/90]$ for the present study. Each layer of the composite had a 3 mm thickness. The composite specimen was considered with the fibre loading mentioned in Table 1. The E-Glass fibre and epoxy resin properties were taken from the literature.

Table 1 Properties of the material

	E (GPa)	Poisson's ratio, ν	Vol. %
E-Glass	70	0.22	65
Epoxy	2.5	0.3	35

2.1 Analytical Methods for the prediction of interlaminar stresses

a) Classical Lamination Plate Theory (CLPT)

The properties of the composite specimen considered in all three directions were calculated using the mixture rule. Then, the stiffness matrices for each lamina have been formulated as follows:

$$Q_{ij} = \begin{bmatrix} Q_{11} & Q_{12} & 0 \\ Q_{21} & Q_{22} & 0 \\ 0 & 0 & Q_{66} \end{bmatrix} \quad (1)$$

Where,

$$Q_{11} = \frac{E_{11}}{(1-\nu_{12}\nu_{21})}; \quad (2)$$

$$Q_{12} = \frac{\nu_{12}E_{11}}{(1-\nu_{12}\nu_{21})}; \quad (3)$$

$$Q_{22} = \frac{E_{22}}{(1-\nu_{12}\nu_{21})}; \text{ and} \quad (4)$$

$$Q_{66} = G_{12} \quad (5)$$

The above-derived stiffness matrix is for the laminate having 0° ply orientation. So, hence, the following relationships are used to derive the stiffness matrices for the other orientations.

$$[\bar{Q}_{ij}]_\theta = \begin{bmatrix} \bar{Q}_{11} & \bar{Q}_{12} & \bar{Q}_{13} \\ \bar{Q}_{21} & \bar{Q}_{22} & \bar{Q}_{23} \\ \bar{Q}_{31} & \bar{Q}_{32} & \bar{Q}_{66} \end{bmatrix} \quad (6)$$

Where,

$$\bar{Q}_{11} = Q_{11}C^4 + Q_{22}S^4 + 2(Q_{12} + 2Q_{66})S^2C^2 \quad (7)$$

$$\bar{Q}_{12} = \bar{Q}_{21} = (Q_{11} + Q_{22} - 4Q_{66})S^2C^2 + Q_{12}(C^4 + S^4) \quad (8)$$

$$\bar{Q}_{13} = \bar{Q}_{31} = (Q_{11} - Q_{12} - 2Q_{66})C^3S - (Q_{22} - Q_{12} - 2Q_{66})S^3C \quad (9)$$

$$\bar{Q}_{22} = Q_{11}S^4 + Q_{22}C^4 + 2(Q_{12} + 2Q_{66})S^2C^2 \quad (10)$$

$$\bar{Q}_{23} = \bar{Q}_{32} = (Q_{11} - Q_{12} - 2Q_{66})CS^3 - (Q_{22} - Q_{12} - 2Q_{66})C^3S \quad (11)$$

$$\bar{Q}_{66} = (Q_{11} + Q_{22} - 2Q_{12} - 2Q_{66})S^2C^2 + Q_{66}(S^4 + C^4) \quad (12)$$

After deriving the stiffness matrices for the entire structure, three special type of stiffness matrices have been formed namely [A] (extensional stiffness matrix), [B] (Bending stiffness matrix) and [D] (coupling stiffness matrix).

$$[A] = \sum_{k=1}^n [Q]_k [h_k - h_{k-1}] \quad (13)$$

$$[B] = \frac{1}{2} \sum_{k=1}^n [Q]_k [h_k^2 - h_{k-1}^2] \quad (14)$$

$$[D] = \frac{1}{3} \sum_{k=1}^n [Q]_k [h_k^3 - h_{k-1}^3] \quad (15)$$

After the formulation of the [A], [B] and [D] matrices, the derived form of the following equation was used to obtain the required strain matrix.

$$\begin{bmatrix} \varepsilon_{xx} \\ \varepsilon_{yy} \\ \gamma_{xy} \end{bmatrix} = [A_1] \begin{bmatrix} N_{xx} \\ N_{yy} \\ N_{xy} \end{bmatrix} + [B_1] \begin{bmatrix} k_{xx} \\ k_{yy} \\ k_{xy} \end{bmatrix} \quad (16)$$

With the assumption of mid-plane curvature being zero about the mid-plane, the above equation got reduced to:

$$\begin{bmatrix} \varepsilon_{xx} \\ \varepsilon_{yy} \\ \gamma_{xy} \end{bmatrix} = [A_1] \begin{bmatrix} N_{xx} \\ N_{yy} \\ N_{xy} \end{bmatrix} \quad (17)$$

$$\text{Where, } [A_1] = [A^{-1}] + [A^{-1}BD^{*-1}BA^{-1}] \quad (18)$$

$$[D^*] = [D] - [BA^{-1}B] \quad (19)$$

Hook's law was used to get the stress matrix.

$$\begin{bmatrix} \sigma_{xx} \\ \sigma_{yy} \\ \tau_{xy} \end{bmatrix} = [Q] \begin{bmatrix} \varepsilon_{xx} \\ \varepsilon_{yy} \\ \gamma_{xy} \end{bmatrix} \quad (20)$$

3.2 Higher Order Lamination Plate Theory

The higher-order lamination Plate Theory formulated with the consideration of the warping deformation effect was considered for the prediction of interlaminar stress and free-edge stress in the proposed composite plate [1, 2].

$$\begin{aligned} \sigma_y(y, z) = & \{-C_{yy}v_{xy}^{eff} - C_{yz}v_{xz}^{eff}\} \varepsilon_x^0 + \\ & C_{yy}\{k_1P_1 - \lambda_2\mu k_2P_2e^{-\lambda_2\mu y} - \\ & \lambda_3\mu k_3P_3e^{-\lambda_3\mu y}\} + \{(-C_{yy}\lambda_2\mu k_2Q_2 + \\ & C_{yz}\mu k_2R_2)e^{-\lambda_2\mu y} + (-C_{yy}\lambda_3\mu k_3Q_3 + \\ & C_{yz}\mu k_3R_3)e^{-\lambda_3\mu y}\} \cos \mu z \end{aligned} \quad (21)$$

3. Numerical analysis of interlaminar stresses

The known mechanical properties have been used as the input data for the analysis. The interlaminar stress induced in the considered E-Glass epoxy composite specimen has been analyzed using ANSYS software. For the given load of 1000 N/mm, the stress distribution along the composite laminate was successfully read out.

4. Results and Discussion

5.1. Analytical Study Results

The induced interlaminar stress in the composite plate was predicted with the aid of the analytical approaches viz. CLPT and HLPT are presented in Tables 2 and 3, respectively.

Table 2 CLPT Inter-laminar stress results under 1000 N/mm loading

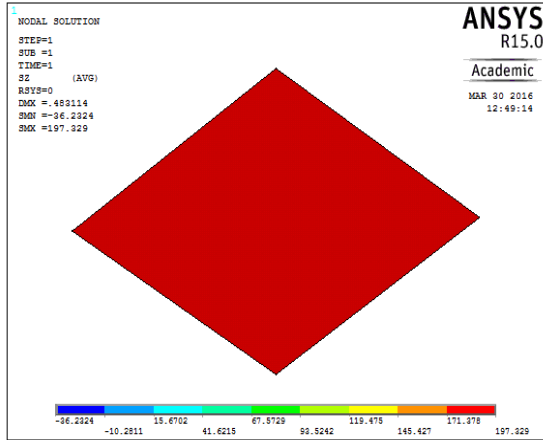
S. No.	Between 0°/30° layer (MPa)	Between 30°/60° layer (MPa)	Between 60°/90° layer (MPa)
1.	319.1856	120.0339	21.1286

Table 3 HLPT Inter-laminar stress results under 1000 N/mm loading

S. No.	Between 0°/30° layer (MPa)	Between 30°/60° layer (MPa)	Between 60°/90° layer (MPa)
1.	322.0135	123.0001	22.9996

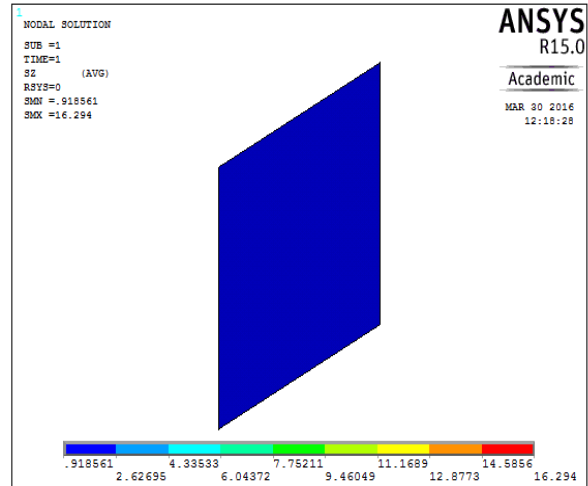
5.2 Numerical Analysis Results

The stress distribution in the 0°, 30°, 60° and 90° laminates for the considered loading condition are shown in figures 1, 2, 3 and 4 respectively. The average stress value induced in the 0° and the 30° laminates was considered to be the interlaminar stress between the 0°/30° laminates. Similarly, the interlaminar stress values acting between the 30°/60° and 60°/90° laminates have been calculated; and the predicted stress values are presented in Table 4.



ELEMENT=	8194	SHELL181					
NODE	SX	SY	SZ	SKY	SVZ	SKZ	
8480	-258.94	-0.66159E-29	-36.232	0.12383E-12	-0.18480E-12	34.239	
8499	-258.94	-0.66159E-29	-36.232	0.12383E-12	-0.18480E-12	34.239	
8500	-258.94	-0.66159E-29	-36.232	0.12383E-12	-0.18480E-12	34.239	
8481	-258.94	-0.66159E-29	-36.232	0.12383E-12	-0.18480E-12	34.239	
8480	43.174	0.64499E-30	197.33	0.54706E-15	0.99864E-14	-34.239	
8499	43.174	0.64499E-30	197.33	0.54706E-15	0.99864E-14	-34.239	
8500	43.174	0.64499E-30	197.33	0.54706E-15	0.99864E-14	-34.239	
8481	43.174	0.64499E-30	197.33	0.54706E-15	0.99864E-14	-34.239	

Fig. 2 Stress distribution in the 30° lamina for 1000 N/mm loading condition



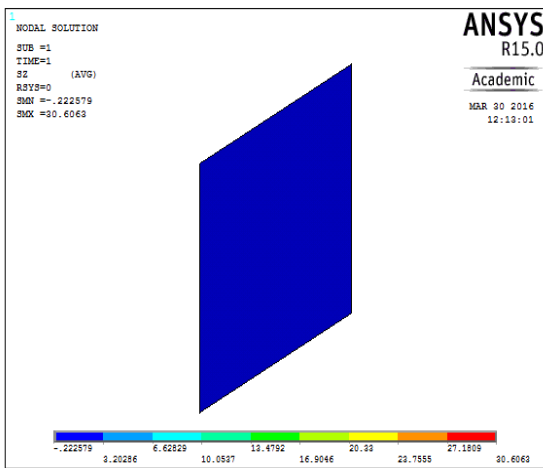
ELEMENT=	471	SHELL181					
NODE	SX	SY	SZ	SKY	SVZ	SKZ	
213	0.59375E-31	106.05	0.91856	0.12063E-13	-1.9352	-0.51295E-15	
510	0.59375E-31	106.05	0.91856	0.12063E-13	-1.9352	-0.51295E-15	
511	0.59375E-31	106.05	0.91856	0.12063E-13	-1.9352	-0.51295E-15	
214	0.59375E-31	106.05	0.91856	0.12063E-13	-1.9352	-0.51295E-15	
213	0.61093E-31	-14.701	16.294	-0.11850E-15	1.9352	-0.99772E-15	
510	0.61093E-31	-14.701	16.294	-0.11850E-15	1.9352	-0.99772E-15	
511	0.61093E-31	-14.701	16.294	-0.11850E-15	1.9352	-0.99772E-15	
214	0.61093E-31	-14.701	16.294	-0.11850E-15	1.9352	-0.99772E-15	

Fig. 4 Stress distribution in the 90° lamina for 1000 N/mm loading condition

Table 4 Numerical interlaminar stress results under 1000 N/mm loading

S. No.	Between 0°/30° lamina (MPa)	Between 30°/60° lamina (MPa)	Between 60°/90° lamina (MPa)
	1.	332.887	123.9677

The results of all the proposed approaches have been obtained. The interlaminar stress results obtained from the analytical and numerical analyses have been compared and presented in Table 5. The numerical analysis results were found to be in agreement with those of the CLPT and the HLPT results.



ELEMENT=	581	SHELL181					
NODE	SX	SY	SZ	SKY	SVZ	SKZ	
585	-0.35605E-30	135.71	-0.22258	-0.16872E-13	2.8781	0.29142E-14	
84	-0.35605E-30	135.71	-0.22258	-0.16872E-13	2.8781	0.29142E-14	
85	-0.35605E-30	135.71	-0.22258	-0.16872E-13	2.8781	0.29142E-14	
586	-0.35605E-30	135.71	-0.22258	-0.16872E-13	2.8781	0.29142E-14	
585	0.11476E-30	-18.515	30.606	0.17623E-15	-2.8781	-0.18741E-14	
84	0.11476E-30	-18.515	30.606	0.17623E-15	-2.8781	-0.18741E-14	
85	0.11476E-30	-18.515	30.606	0.17623E-15	-2.8781	-0.18741E-14	
586	0.11476E-30	-18.515	30.606	0.17623E-15	-2.8781	-0.18741E-14	

Fig. 3 Stress distribution in the 60° lamina for 1000 N/mm loading condition

Table 5 Comparison of the interlaminar stress values calculated by the proposed methods

	Between 0°/30° lamina (MPa)	Between 30°/60° lamina (MPa)	Between 60°/90° lamina (MPa)
CLPT Results	319.1856	120.0339	21.1286
HLPT Results	322.0135	123.0001	22.9996
Numerical Results	332.887	123.9677	23.4502

5. Conclusion

In the present study, the interlaminar stresses induced in an angle ply E-Glass composite plate have been calculated for the loading condition 1000 N/mm with the help of Classical Lamination Plate Theory (CLPT) and Higher Order Lamination Plate Theory (HLPT).

Using ANSYS software, the interlaminar stresses acting in the E-Glass epoxy composite plate under the specified loading condition have been evaluated. The results obtained using ANSYS software justified the results obtained from the Higher-order theory. As classical lamination theory was used to derive the Higher-order lamination theory, including warping deformation mode, the results obtained using HLPT will improve and be more accurate than all other existing theoretical methods. Hence, the ANSYS results ensured that Higher-order Lamination Plate Theory (HLPT) improved accuracy over Classical Lamination Plate Theory (CLPT).

References

1. S. Ramaswamy, J. Selwin Rajadurai, and A. Arul Marcel Moshi, "Prediction of free edge stresses in the composite laminates and its validation through experimental means," *International Journal of Advanced Research Trends in Engineering and Technology (IJARTET)*, vol. 1, no. 1, pp. 11–17, 2014.
2. S. Ramaswamy, A. Arul Marcel Moshi, and J. Selwin Rajadurai, "Effect of Warping Deformation mode in the Prediction of Free Edge stresses in the composite laminates," *International Journal of Applied Engineering Research (IAER)*, vol. 10, no. 8, pp. 223–229, 2015.
3. S. Ramaswamy, J. Selwin Rajadurai, and A. Arul Marcel Moshi, "Comparative analysis on classical laminated plate theory and higher order lamination plate theory for cross-ply FRP composite structures," *Journal of Computational and Theoretical Nanoscience*, vol. 14, no. 10, pp. 5444–5449, 2017. DOI: 10.1166/jctn.2017.6968
4. S. Ramaswamy, J. Selwin Rajadurai, and A. Arul Marcel Moshi, "Software analysis on free edge stresses in the composite laminates using various approaches and its applications," *Applied Mathematics and Information Sciences*, vol. 13, no. 2S, pp. 297–302, 2019. DOI: 10.18576/amis/13S133
5. M. Tahani and A. Nosier, "Three-dimensional interlaminar stress analysis at free edges of general cross-ply composite laminates," *Materials and Design*, vol. 24, no. 2, pp. 121–130, 2003. DOI: 10.1016/S0261-3069(02)00107-3
6. M. Tahani, "Analysis of laminated Composite beams using layer wise displacement theories," *Composite Structures*, vol. 79, no. 4, pp. 535–547, 2007. DOI: 10.1016/j.compstruct.2006.02.019
7. A. Nosier and M. Maleki, "Free-edge stresses in general composite laminates," *International Journal of Mechanical Sciences*, vol. 50, no. 7, pp. 1435–1447, 2008. DOI: 10.1016/j.ijmecsci.2008.09.002
8. H. Yazdani Sarvestani and M. Yazdani Sarvestani, "Interlaminar stress analysis of general composite laminates," *International Journal of Mechanical Sciences*, vol. 53, no. 7, pp. 958–967, 2011. DOI: 10.1016/j.ijmecsci.2011.07.007
9. T. Kant and B. S. Manjunatha, "Higher Order theories for symmetric and unsymmetric fiber reinforced composite beams with CO Finite Elements," *Finite Elements in Analysis and Design*, vol. 6, no. 4, pp. 303–320, 1990. DOI: 10.1016/0168-874X(90)90022-7
10. J. Lindemann and W. Becker, "Analysis of the free-edge effect in composite laminates by the boundary finite element method," *Mechanics of Composite Materials*, vol. 36, no. 3, pp. 207–214, 2000. DOI: 10.1007/BF02681872
11. M. Tahani and A. Nosier, "Edge effects of uniformly loaded cross-ply composite laminates," *Materials and Design*, vol. 24, no. 8, pp. 647–658, 2003. DOI: 10.1016/S0261-3069(03)00098-0
12. T. Kant and S. M. Shiyekar, "An assessment of a higher order theory for composite laminates subjected to thermal gradient," *Composite structures*, vol. 96, pp. 698–707, 2013. DOI: 10.1016/j.compstruct.2012.08.045